Design And Performance Analysis Of A New Uncoupled Radial Hybrid Magnetic Bearing

Jun Liu[1], Xiaojun Lin[2*], Xinquan Yin[3], and Juanjuan Qin[2]

[1] Lanzhou Institute of Technology, School of Civil Engineering, Lanzhou, Gansu, China 730050
[2] Lanzhou Institute of Technology, School of Mechatronics Engineering, Lanzhou, Gansu, China 730050
[3] Lanzhou Institute of Technology, School of Automotive Engineering, Lanzhou, Gansu, China 730050
[*] Corresponding author. E-mail: lljjlljj2023@163.com

Received: Jun. 04, 2023; Accepted: Sept. 23, 2023

There is a coupling problem between the bias magnetic circuit and the control magnetic circuit of hybrid magnetic levitation bearings, which not only affects the support stiffness of the magnetic bearing, but also increases the difficulty of control and power consumption. To solve this problem, an uncoupled radial hybrid magnetic bearing (RHMB) with four stator cores in the front and rear rows is proposed, which achieves the design of independent magnetic circuit channels for bias magnetic field and control magnetic field. Subsequently, an equivalent magnetic circuit model for the new magnetic bearing was established and its electromagnetic force analytical calculation formula was derived. In order to verify the performance of the new structure and the effectiveness of the analytical model, the ANSYS Electronics Desktop software was used to simulate and analyze its three-dimensional magnetic field distribution, electromagnetic force variation patterns, and coupling characteristics. The results show that the proposed analytical model for the new structure is effective and can effectively linearize the force displacement and force current relationships, which is consistent with the calculation results of the simulation model. In addition, compared to traditional structures, the new structure has better magnetic field decoupling characteristics, which can reduce the eddy current loss of the iron core by 50.12% and the required control current from 2.3A to 1A. The research results can provide theoretical basis for the design and control of magnetic levitation bearings.

Keywords: Radial hybrid magnetic bearing; Independent magnetic circuits; Analytic calculation; Decoupling; Finite element analysis

© The Author('s). This is an open-access article distributed under the terms of the Creative Commons Attribution License (CC BY 4.0), which permits unrestricted use, distribution, and reproduction in any medium, provided the original author and source are cited.

http://dx.doi.org/10.6180/jase.202408_27(8).0012

1. Introduction

Magnetic bearings are a new type of bearings that suspend the shaft without mechanical contact by using the controllable magnetic force. They are characterized by advantages including no friction and mechanical wear, no need for lubrication and sealing, high speed, and long service life, and therefore have been widely applied to industrial fields including flexible rotor, aerospace, medical facility, flywheel energy storage, and turbomachinery [1–4]. Magnetic bearings generally can be classified into three types: active magnetic bearings, passive permanent-magnet bearings, and hybrid magnetic bearings. The bias and control magnetic fluxes of active magnetic bearings are both generated by control coils, which can actively control the stiffness, damping, and rotor displacement of bearings, while such bearings also have an obvious shortcoming of high power consumption [5–7]. Passive permanent-magnet bearings do not have power consumption and show a simple structure. However, they also have poor stability and uncontrollable magnetic force. Hybrid magnetic bearings, which combine

advantages of the above two, provide the bias magnetic flux using permanent magnets. This reduces excitation power consumption of bearing systems and controls the volume and mass of circuits, so hybrid magnetic bearings have received increasingly more attention from researchers [8, 9].

Researchers have conducted numerous studies on hybrid magnetic bearings. Hossain [10] proposed a radial hybrid magnetic bearing (RHMB) with two radial stators that is applied to high-temperature conditions. Each stator has six poles and the permanent magnets are used for radial magnetization and sticked on the outer circle of poles of radial stators. Jingyun [11] designed the topology of an uncoupled RHMB, in which the circular permanent magnet is used for axial magnetization and independent stator cores in X and Y directions are adopted. Moreover, the coupling performance of the RHMB was also verified through simulation and tests. Zong et al. [12] studied the coupling of radial 2 degrees of freedom (DOFs) of a four-pole hybrid magnetic bearing, and proposed the feed-forward decoupling control strategy and the feed-forward compensator decoupling method. Zhong Zhixian, Cai Zhonghou [13] came up with a new four-pole RHMB with six independent magnetic circuits and overcame the magnetic circuit coupling of magnetic bearings from the perspective of mechanical structures.

Based on previous research, the current research proposed a new uncoupled RHMB, in which independent stator cores in x and y directions were both used in the front and rear rows. In addition, independent magnetic circuits of bias and control magnetic fields were designed. An equivalent magnetic circuit model was also established for the RHMB and the analytical calculation formula for its electromagnetic force was derived. Moreover, a finite element simulation model was built using the ANSYS Electronics Desktop software. Then, the three-dimensional (3D) magnetic field distribution, force-displacement and force-current relationships, and coupling characteristics of different magnetic fields under different excitation conditions were analyzed. Calculation and simulation results indicate that the new RHMB designed in the research can effectively overcome the radial magnetic circuit coupling through appropriate design of the mechanical structure.

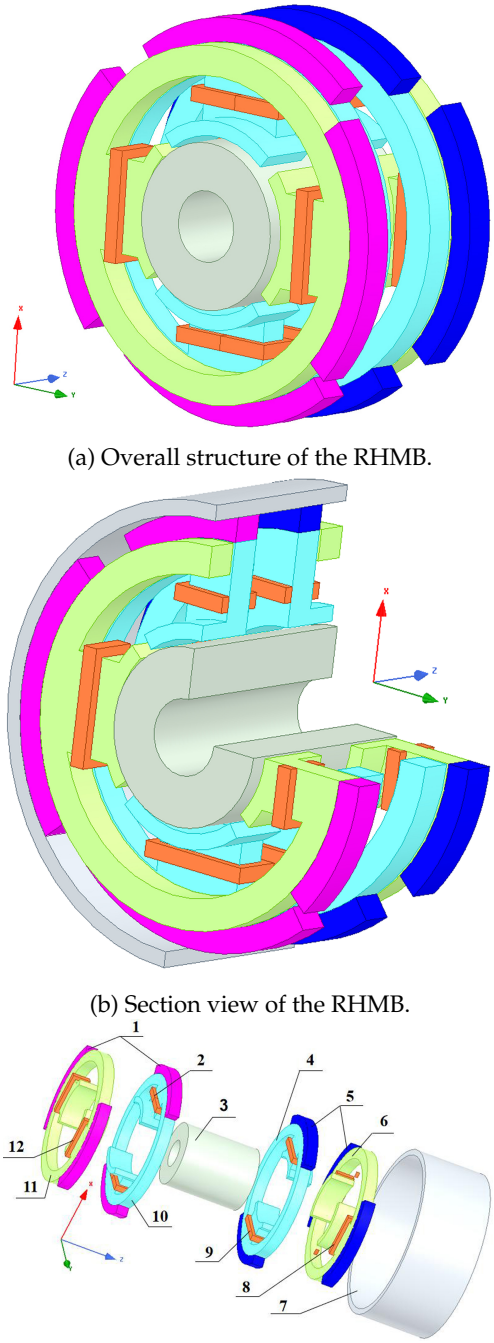

(a) Overall structure of the RHMB.

(b) Section view of the RHMB.

(c) Structural decomposition of the RHMB.

Fig. 1. Structure of the new uncoupled RHMB. 1-Permanent magnets; 2-x_f control coils; 3-Rotor core; 4-x_r stator cores; 5-Permanent magnets; 6-y_r stator cores; 7-Outer stator core; 8-y_r control coils; 9-xr control coils; 10-x_f stator cores; 11-y_f stator cores; 12-y_f control coils.

2. Structure and working principle of the new uncoupled rhmb

2.1. Structure of the new uncoupled RHMB

The structure of the new uncoupled RHMB is shown in Fig. 1. It is composed of the hybrid magnetic bearing components in the front and rear rows, a rotor core, and an outer stator core. The hybrid magnetic bearing components in the front row include the x_f stator cores and x_f

control coils installed on their two poles, y_f stator cores and yf control coils installed on their two poles, and four permanent magnets corresponding to the poles. Among them, the x_f control coils produce the control magnetic flux in the x direction; y_f control coils produce the control magnetic flux in the y direction; permanent magnets produce the bias magnetic flux; x_f and y_f stator cores are independent, so that control and bias magnetic fluxes (two of each) in radial x and y directions both have independent magnetic circuits; the four poles on x_f and y_f stator cores are designed to be a coplanar structure about xy central plane and they are uniformly distributed with an angle of 90° to ensure axial equilibrium of the radial suspension force; permanent magnets corresponding to poles are installed in a coplanar manner about xy central plane with their corresponding stator cores, and the four permanent magnets are used for radial magnetization, with the N pole pointing inwards. The hybrid magnetic bearing components in the rear row basically share the same structure with that in the front row, while the difference lies in that the four permanent magnets are used for radial magnetization, with the N pole pointing outwards.

2.2. Magnetic circuits and working principle of the RHMB

The bias magnetic fluxes generated by the permanent magnets are indicated by dotted lines with arrows in Fig. 2 (a). In the figure, the bias magnetic flux in the x+ direction departs from the N pole of the front-row permanent magnet, then passes through x_f stator, air gap, rotor core, air gap, x_r stator, rear-row permanent magnet, air gap, and outer stator core, and finally returns to the S pole of front-row permanent magnet, to form a closed path. The bias magnetic flux in the y+ direction starts from the N pole of front-row permanent magnet, then passes through y_f stator, air gap, rotor core, air gap, y_r stator, rear-row permanent magnet, air gap, and outer stator core, and finally returns to the S pole of front-row permanent magnet, to form a closed path as well. The bias magnetic flux paths in x- and y- directions are also same as the above analysis. By designing the locations of stator cores in x and y directions and of permanent magnets in front and rear rows, Fig. 2 (a) shows that four bias magnetic flux paths in x+, x-, y+, and y- directions are independent in the radial direction and are decoupled.

Control coils produce control fluxes. The magnetic fluxes of hybrid magnetic bearings in the front and rear rows are illustrated in Fig. 2 (b), in which control fluxes in x_f, x_r, y_f, and y_r directions separately represent magnetic fluxes produced by radial windings at poles of stator cores in x and y directions in front and rear rows. Due to the large magnetic resistance of permanent magnets, the control magnetic flux path does not pass through the permanent magnets. As a result, control and bias magnetic fluxes are decoupled, which decreases power consumption and avoids demagnetization of permanent magnets.

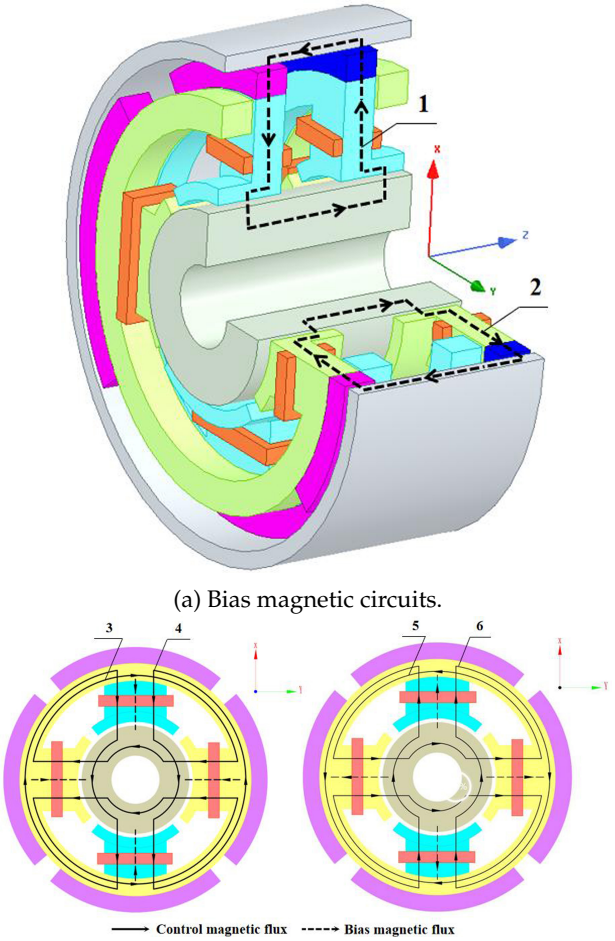

(a) Bias magnetic circuits.

(b) Hybrid magnetic circuits.

Fig. 2. Schematic diagram for magnetic circuits of the uncoupled RHMB. 1-Bias magnetic flux in x+ direction; 2-Bias magnetic flux in y+ direction; 3-Control magnetic flux in the y_f direction; 4-Control magnetic flux in the x_f direction; 5-Control magnetic flux in the yr direction; 6-Control magnetic flux in the x_r direction.

The four bias magnetic fluxes generated by permanent magnets can produce the attractive force between the stator and rotor, which is separately symmetrical in x and y directions. If not considering the gravity, the radial resultant force on the rotor induced by bias magnetic fluxes is zero. If there is no external interference and control coils are not powered on, the rotor is located at the central balance position and remains stably suspended. The working principle of the new uncoupled RHMB was analyzed taking x axis

as an example. When a load in the x- direction is applied to the rotor, the rotor has displacement in the x- direction, the air gap in the x- direction narrows, and the magnetic field intensity is enhanced; the air gap in the x+ direction enlarges, and magnetic field intensity reduces, which impairs the balance of the rotor. Under the condition, the control coil in the x direction is powered on to allow the current in the x direction to produce control magnetic fluxes at the air gap. The control magnetic flux in the x+ direction is in the same direction as the bias magnetic flux, so the magnetic forces are superposed; the control magnetic flux in the x- direction is in the opposite direction as the bias magnetic flux, so the magnetic forces are offset. As a result, a resultant force in the magnetic field in the x+ direction is generated, which enables the rotor to return to the balance position.

3. Structure parameter design calculation and performance analysis of of the new uncoupled rhmb

3.1. Structural Design and Main sizing Equation

To reduce the coupling effect between different magnetic fields and poles, both the front and rear stator poles are selected as 4 poles. The stator coil slots are adopted rectangular slots. Assuming that the main shaft diameter of a rotating mechanical device is d_0, it is necessary to design and determine other structural parameters [14–16].

Stator inner diameter D

$$D = d + 2l_g \tag{1}$$

where d is outer diameter of the rotor; l_g is the radial air gap at the rotor balance position.

Arc length of the pole shoe l_a

$$l_a = \lambda \frac{\pi D}{2P} \tag{2}$$

where λ ranges from 0.7 to 0.9; P is number of pole pairs.

Pole width l_w

$$l_w = \varsigma l_a \tag{3}$$

where ς ranges from 0.8 to 1.

Thickness of rotor core l_w

$$l_r \geq \frac{(2l_g + d_0)\,\pi\lambda\varsigma}{2(P - \pi\lambda\varsigma)} \tag{4}$$

Coil turns n

$$n = \frac{2B_{\max} l_g}{\mu_0 I_{\max}} \tag{5}$$

where $B_{\max}$ is the maximum magnetic density excited at the air gap when the control coil is energized; $I_{\max}$ is the maximum current that the power amplifier can provide to the control. coil.

3.2. Establishment of the equivalent magnetic circuit model and calculation of the electromagnetic force

When ignoring the magnetic resistances of stator and rotor cores, saturation of magnetic circuits, magnetic flux leakage, and vortex effect while only allowing the bias magnetic flux to work, the equivalent magnetic circuit is displayed in Fig. 3. In the figure, R_m is the magnetic resistance of permanent magnets; F_m is the magnetomotive force of permanent magnets; $\phi_{fx+}, \phi_{rx+}, \phi_{fy+}, \phi_{ry+}, \phi_{fx-}, \phi_{rx-}, \phi_{fy-}$, and ϕ_{ry-} separately represent the bias magnetic fluxes produced by eight permanent magnets in the front and rear rows; $R_{fx+}, R_{rx+}, R_{fy+}$, $R_{ry+}, R_{fx^-}, R_{rx-}, R_{fy^-}$, and R_{ry-} separately denote magnetic resistances of air gaps between stator and rotor cores along x and y directions of hybrid magnetic bearings in the front and rear rows; $\phi_{pfx+}, \phi_{prx+}, \phi_{pfy+}, \phi_{pry+}, \phi_{pfx-}, \phi_{prx-}, \phi_{pfy-}$, and ϕ_{pry-} are bias magnetic fluxes at air gaps. Because independent structures are used for two stator cores separately in the x and y directions, the control magnetic circuits are non-interfering. The equivalent magnetic circuits are shown in Fig. 4 when only the control magnetic flux works. In the figure, Ni_{fx+},, Ni_{fx-}, $Ni_{fy+}, Ni_{fy-}, Ni_{rx+}, Ni_{rx-}, Ni_{ry+}$, and Ni_{ry-} are separately magneto motive forces produced by control coils on stator cores along x and y directions of hybrid magnetic bearings in the front and rear rows; $\phi_{cfx+}, \phi_{cfx-}, \phi_{cfy+}, \phi_{cfy-}, \phi_{crx+}, \phi_{crx-}, \phi_{cry+}$, and ϕ_{cry-} are control magnetic fluxes at air gaps.

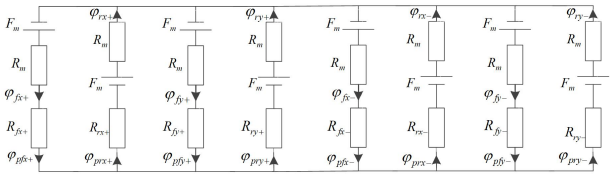

Fig. 3. The equivalent magnetic circuits when only considering the bias magnetic flux.

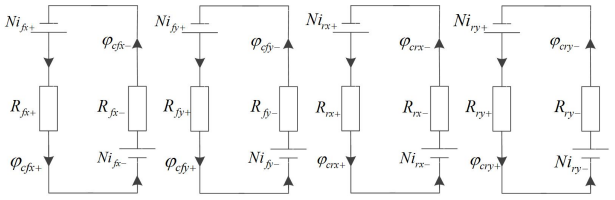

Fig. 4. The equivalent magnetic circuits when only considering the control magnetic flux.

The magnetic resistance of permanent magnets is

$$R_m = l_m / \mu_m S_m \tag{6}$$

where l_m is the thickness of permanent magnets along the radial direction; μ_m is magnetic conductivity of permanent magnets; S_m is the area of permanent magnets along the peripheral direction.

The magnetic resistance of air gaps is

$$\begin{cases} R_{fx+} = R_{rx+} = \frac{l_g - \delta_x}{\mu_0 S}, R_{fy_+} = R_{ry+} = \frac{l_g - \delta_y}{\mu_0 S} \\ R_{fx-} = R_{rx-} = \frac{l_g + \delta_x}{\mu_0 S}, R_{fy_-} = R_{ry-} = \frac{l_g + \delta_y}{\mu_0 S} \end{cases} \tag{7}$$

where l_g is the radial length of air gaps at the rotor balance position; δ_x is the displacement in the $x+$ direction; δ_y is the displacement in the $y+$ direction; μ_0 is magnetic conductivity of air; S is the area of radial poles.

The magnetic resistances of the four bias magnetic circuits are

$$\begin{cases} R_{x+} = 2R_m + R_{fx+} + R_{rx+} \\ R_{x-} = 2R_m + R_{fx-} + R_{tx-} \\ R_{y+} = 2R_m + R_{fy_+} + R_{ry+} \\ R_{y-} = 2R_m + R_{fy_-} + R_{ry-} \end{cases} \tag{8}$$

The bias magnetic fluxes of the four corresponding permanent magnetic circuits are

$$\begin{cases} \varphi_{fx+} = \varphi_{rx_+} = 2F_m / R_{x+} \\ \varphi_{fx-} = \varphi_{rx_-} = 2F_m / R_{x-} \\ \varphi_{fy+} = \varphi_{ry+} = 2F_m / R_{y+} \\ \varphi_{fy-} = \varphi_{ry-} = 2F_m / R_{y-} \end{cases} \tag{9}$$

The bias magnetic fluxes at the air gaps of poles are [17]

$$\begin{cases} \varphi_{pfx+} = \varphi_{prx+} = \varphi_{fx+} / \varepsilon_{x+} \\ \varphi_{pfy+} = \varphi_{pry+} = \varphi_{fy+} / \varepsilon_{y+} \\ \varphi_{pfx-} = \varphi_{prx-} = \varphi_{fx-} / \varepsilon_{x-} \\ \varphi_{pfy-} = \varphi_{pry-} = \varphi_{fy-} / \varepsilon_{y-} \end{cases} \tag{10}$$

where $\varepsilon_{x+}, \varepsilon_{x-}, \varepsilon_{y+}$, and ε_{y-} denote the magnetic leakage factors of poles in $x+, x-, y+$, and y-directions.

The control magnetic fluxes produced by control coils are

$$\begin{cases} \varphi_{cfx+} = \varphi_{cfx-} = Ni_{fx+} \mu_0 S / l_g \\ \varphi_{cfy+} = \varphi_{cfy-} = Ni_{fy+} \mu_0 S / l_g \\ \varphi_{crx+} = \varphi_{crx-} = Ni_{rx+} \mu_0 S / l_g \\ \varphi_{cry+} = \varphi_{cry-} = Ni_{ry+} \mu_0 S / l_g \end{cases} \tag{11}$$

Then, there are

$$\begin{cases} \varphi_{cx} = \varphi_{cfx+} + \varphi_{crx+} \\ \varphi_{cy} = \varphi_{cfy+} + \varphi_{cry+} \end{cases} \tag{12}$$

where φ_{cx} and φ_{cy} are separately total control magnetic fluxes in the x and y directions.

The resultant magnetic flux at the air gaps can be calculated by combining Eqs. (10) and (11).

$$\begin{cases} \Phi_{fx+} = \varphi_{pfx+} + \varphi_{cfx+}, \Phi_{fx-} = \varphi_{pfx+} - \varphi_{cfx-} \\ \Phi_{fy+} = \varphi_{pfy+} + \varphi_{cfy+}, \Phi_{fy-} = \varphi_{pfy+} - \varphi_{cfy-} \\ \Phi_{rx+} = \varphi_{prx-} + \varphi_{crx+}, \Phi_{rx-} = \varphi_{prx-} - \varphi_{crx-} \\ \Phi_{ry+} = \varphi_{pry-} + \varphi_{cry+}, \Phi_{ry-} = \varphi_{pry-} - \varphi_{cry+} \end{cases} \tag{13}$$

Then, there are

$$\begin{cases} \Phi_{x+} = \Phi_{fx+} + \Phi_{rx+}, \Phi_{x-} = \Phi_{fx-} + \Phi_{rx-} \\ \Phi_{y+} = \Phi_{fy+} + \Phi_{ry+}, \Phi_{y-} = \Phi_{fy-} + \Phi_{ry-} \end{cases} \tag{14}$$

where $\Phi_{x+}, \Phi_{x-}, \Phi_{y+}$, and Φ_{y-} separately denote resultant magnetic fluxes in $x+, x-, y+$, and y-directions.

Therefore, the radial magnetic levitation forces in x and y directions can be calculated as:

$$\begin{cases} F_x = \left(\Phi_{x+}^2 - \Phi_{x-}^2\right) / 2\mu_0 S \\ F_y = \left(\Phi_{y+}^2 - \Phi_{y-}^2\right) / 2\mu_0 S \end{cases} \tag{15}$$

If the rotor deviates from the balance position, the allowable displacement is generally very small, which leads to a small difference in the magnetic resistance of air gaps. F_x and F_y can be processed at the rotor balance position, thus obtaining the following linearized mathematical model for the radial suspension forces in the x and y directions of the new uncoupled RHMB.

$$\begin{cases} F_x \approx \left.\frac{\partial F_x}{\partial x}\right|_{\substack{i_x=0 \\ x=y=0}} \cdot x + \left.\frac{\partial F_x}{\partial i_x}\right|_{\substack{i_x=0 \\ x=y=0}} \cdot i_x = K_x \left(x_{fx} + x_{rx}\right) + K_{ix} \left(i_{fx} + i_{rx}\right) \\ F_y \approx \left.\frac{\partial F_y}{\partial y}\right|_{\substack{i_y=0 \\ x=y=0}} \cdot y + \left.\frac{\partial F_y}{\partial i_y}\right|_{\substack{i_y=0 \\ x=y=0}} \cdot i_y = K_y \left(y_{fy} + y_{ry}\right) + K_{iy} \left(i_{fy} + i_{ry}\right) \end{cases} \tag{16}$$

where K_x and K_y separately denote radial force-displacement factors in x and y directions, $K_x = -\frac{F_m^2 \mu_0 S}{2\varepsilon_{x+}\varepsilon_{x-} l_g^3}$ $K_y = -\frac{F_m^2 \mu_0 S}{2\varepsilon_{y+}\varepsilon_y l_g^3}$; K_{ix} and K_{iy-} are radial force-current factors in x and y directions, $K_{ix} = -\frac{F_m N \mu_0 S}{\varepsilon_{x+}\varepsilon_{x-} l_g^2}$ $K_{iy} = -\frac{F_m N \mu_0 S}{\varepsilon_{y+}\varepsilon_{y-} l_g^2}$ and y directions.

4. 3D finite element simulation

To verify whether the structural design is reasonable or not and whether the established magnetic circuit model and the derived calculation formula of electromagnetic force are accurate or not, 3D finite element modeling and simulation were performed for the new uncoupled RHMB [18]. Parameters of the structural model of the RHMB are listed in Table 1.

Table 1. Parameters of the simulation model of the new uncoupled RHMB.

Items	Parameters	Items	Parameters
Material of permanent magnets	Ndfe 30	Outer diameters of stator cores in x and y directions /mm	60
Outer diameter of permanent magnets /mm	68	Inner diameters of stator cores in x and y directions /mm	30
Inner diameter of permanent magnets/mm	60	Thickness of stator cores in x and y directions/mm	10
Thickness of permanent magnets/mm	10	Outer diameter of the rotor/mm	28
Radian of permanent magnets/rad	1.40	Inner diameter of the rotor/mm	12
Number of turns of control coils	100	Air gaps/mm	1

4.1. Magnetic field distribution

The magnetic field distribution under different excitation conditions is obtained by simulation in the environment of ANSYS Electronics Desktop software, as shown in Figs. 5 to 7.

Figure 5 illustrates distribution of the bias magnetic field in the bearing when only permanent magnets work. Fig. 5 (a) shows distribution of magnetic lines of force; Fig. 5 (b) displays the cloud picture of flux density distribution. It can be seen from Fig. 5 that the distribution and direction of magnetic lines of force as well as the flux density distribution are completely same as the bias magnetic circuits designed in Fig. 2 (a). The flux density is high between permanent magnets in the front and rear rows and near the poles of permanent magnets, reaching 1.7 T around, while that in most other areas of the cores is lower than 1.2 T. In addition, the cores are basically not saturated.

Fig. 6 displays distribution of control magnetic fields produced when only the radial control windings at poles work. Fig. 6 (a) shows distribution of magnetic lines of force; Fig. 6 (b) illustrates the cloud picture of flux density distribution. As shown in Fig. 6, the distribution and direction of magnetic lines of force as well as the flux density distribution are completely consistent with the control magnetic circuits designed in Fig. 2 (b). The radial control windings of eight poles separately produce closed magnetic lines of force in four stator cores separately along x and y directions in the front and rear rows according to design requirements for the direction. Additionally, the magnetic lines of force and flux densities inside the four stator cores n x and y directions are independent and not intersected. This further verifies the rationality of structural design for decoupling of control magnetic fields of radial two DOFs in x and y directions. It can be further seen from Fig. 6 that magnetic lines of force and flux densities are distributed

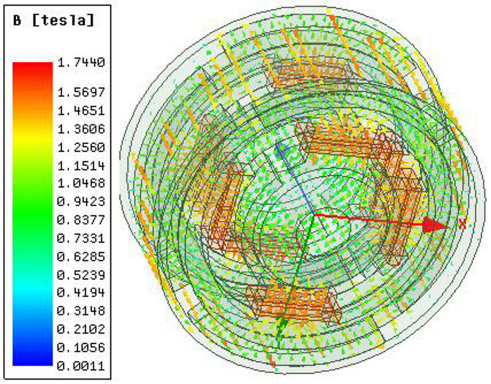

(a) Magnetic lines of force.

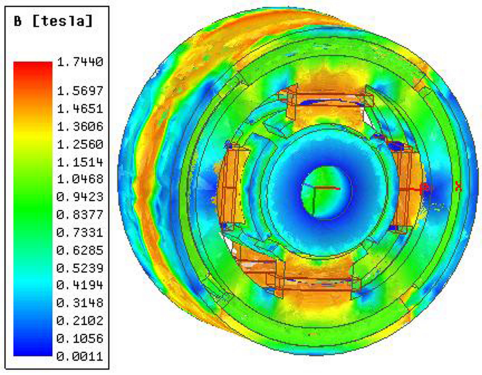

(b) Flux density.

Fig. 5. Bias magnetic fields produced by permanent magnets.

uniformly in the stator cores in x and y directions and in corresponding poles, maintaining at about 1.9 T. A few flux densities with magnetic strength approaching to 0 are distributed outside stator cores in x and y directions, which hardly influence the regulation effect on control magnetic fields. This indicates that the structure is reasonable and

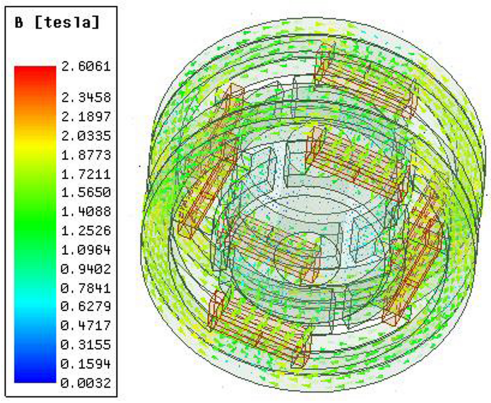

(a) Magnetic lines of force.

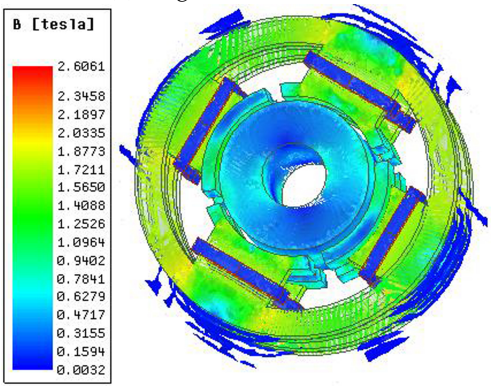

(b) Cloud picture of flux density distribution.

Fig. 6. Control magnetic fields produced by radial control windings at poles.

the magnetic loss is low.

Fig. 7 displays distribution of the hybrid magnetic field in the RHMB when the control magnetic fluxes in x+ and y+ directions produced after switching on radial control windings at poles interact with the bias magnetic field formed by permanent magnets. It can be seen from distribution of magnetic lines of force in Fig. 7 (a) that the magnetic lines of force of control and bias magnetic fluxes along x+ and y+ directions in the front and rear rows are in the same direction, so the magnetic field is enhanced due to superposition of magnetic forces. Whereas, the magnetic lines of force of control and bias magnetic fluxes along x- and y- directions are in the opposite directions, so the magnetic field is weakened due to offset of magnetic forces. The cloud picture for flux density distribution in Fig. 7 (b) further shows that the flux density is high in the superposed magnetic field at poles in x+ and y+ directions in the front and rear rows, reaching 2.2 T; the flux density is low in the offset magnetic field at poles in x- and y- directions in the front and rear rows, with the flux density lower than 0.5 T. This completely meets the design requirements of the new uncoupled RHMB for hybrid magnetic circuits.

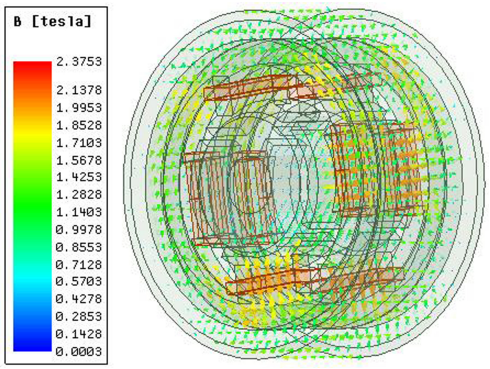

(a) Magnetic lines of force.

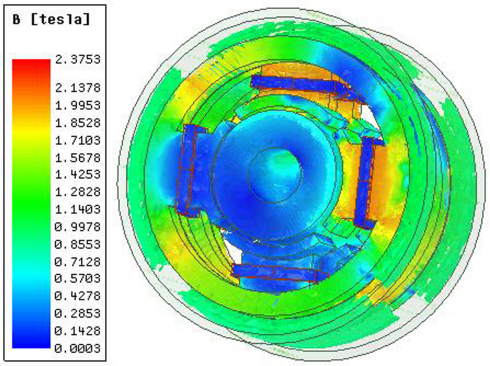

(b) Cloud picture of flux density distribution.

Fig. 7. Distribution of the hybrid magnetic field.

Taking x-direction for example, the flux linkage of winding in x+direction vary with displacement and the x-direction control current, which shown in Fig. 8. It can be seen that the magnetic pole flux linkage gradually increases with the growth of control current; and the magnetic pole flux linkage increases when the magnetic intensity rises with the air gap reducing, the magnetic pole flux linkage decreases when the magnetic intensity weakens with the air gap increasing. Based on the given variation law of magnetic pole flux linkage, it is possible to design reasonably value and direction of the control coil current.

4.2. Simulation of the electromagnetic force

The relationships of the radial electromagnetic force of the new uncoupled RHMB with the rotor displacement and control current of radial windings at poles were obtained via two methods: analytical calculation of the magnetic circuit model and 3D finite element simulation (Figs. 9 and 10). Fig. 9 shows changes in the radial electromagnetic force with rotor displacement in the x direction under conditions without the control current. The analytical calculation results basically remain consistent with the finite element simulation results, with the maximum error of 3.77%. Besides,

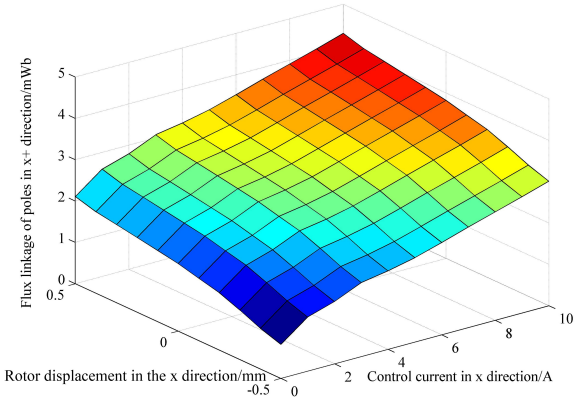

Fig. 8. Diagram of flux linkage.

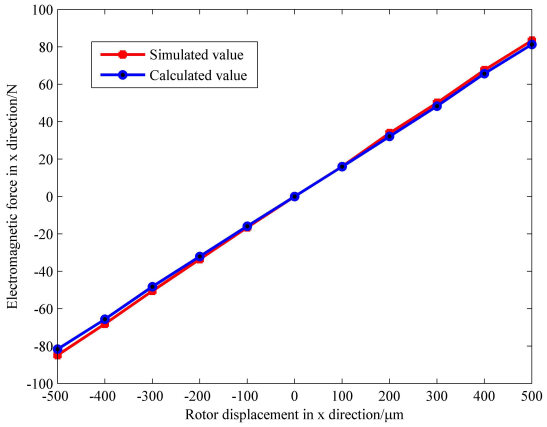

Fig. 9. Variation of the electromagnetic force with the rotor displacement in the x direction.

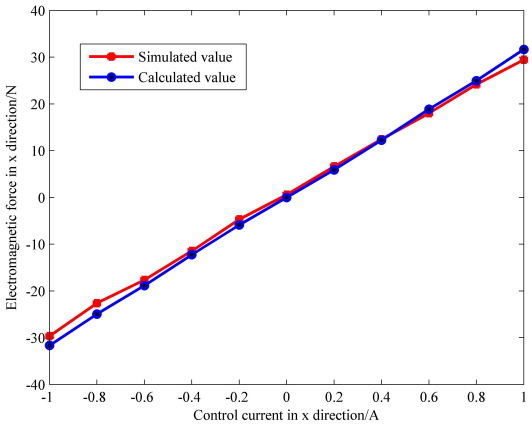

Fig. 10. Variation of the electromagnetic force with the control current in the x direction.

the error enlarges with the increasing rotor displacement. This is possibly because magnetic flux leakage and edge effect of permanent magnets are ignored and some parameters are approximated in the theoretical calculation, so that the electromagnetic force basically linearly changes with the rotor displacement. Fig. 10 displays the relationship between the electromagnetic force and the radial control winding current at poles in the x direction when the rotor is at the balance position, with the maximum error of 6.63%. The analytical calculation results basically agree with the finite element simulation results, and the electromagnetic force basically linearly changes with the control current.

Comprehensive comparison of the analytical calculation and simulation shows that the analytical calculation results using the equivalent magnetic circuit model are basically consistent with the finite element simulation results. The force-displacement and force-current relationships suggest the favorable characteristics of the linear electromagnetic force of the RHMB, which further verifies structural rationality of the designed new RHMB and accuracy of the established magnetic circuit model.

4.3. Coupling of the electromagnetic force

In many structures of traditional radial magnetic bearings, the poles in x and y directions generally share one core, which leads to presence of control magnetic fluxes in x and y directions at the same time in the same pole. Once the rotor deviates from the balance position, the electromagnetic forces in x and y direction are always coupled to different extents, which affects the control precision of magnetic bearings. To solve the problem, independent stator cores in x and y directions are adopted in the designed new RHMB, so that the control magnetic fluxes in x and y directions are independently designed from the perspective of the structure. To study the decoupling performance, 3D finite element simulation was performed to analyze relationships of the electromagnetic force with rotor displacements and the control current in x and y directions, as illustrated in Figs. 11 to 13.

Fig. 11 shows relationships of the electromagnetic force in the x direction with the rotor displacements in x and y directions under conditions that no radial winding current is applied to poles of the RHMB with a new structure. It can be seen from the figure that the electromagnetic force in the x direction is positively proportional to the displacement in the x direction, while the displacement in the y direction hardly affects the electromagnetic force in the x direction. The result indicates that the bias magnetic circuits in x and y directions of the RHMB with the new structure hardly influence each other in x and y directions and they are well

decoupled.

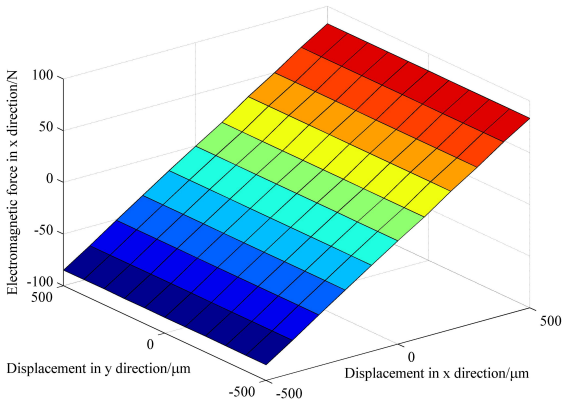

Fig. 11. Variation of the electromagnetic force in the x direction with displacements in x and y directions.

Fig. 12 illustrates the relationships of the electromagnetic force in the x direction with the control currents in x and y directions when the rotor of the RHMB with the new structure is at the balance position. As shown in the figure, the electromagnetic force in the x direction basically has a linear relationship with the control current in the x direction; while the value of control current in the y direction hardly influences the electromagnetic force in the x direction. This suggests that the control magnetic fluxes in x and y directions of the designed RHMB are highly independent and do not influence each other during work, implying the favorable decoupling effect.

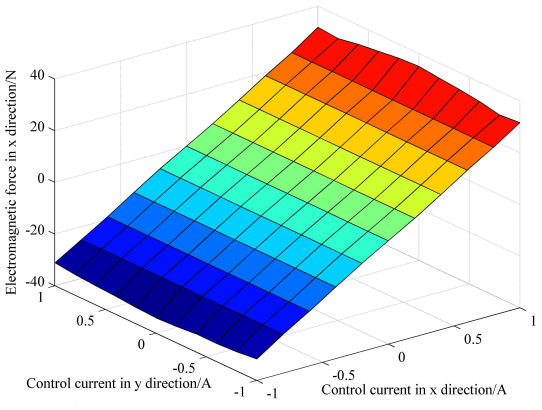

Fig. 12. Variation of the electromagnetic force in the x direction with control currents in x and y directions.

Fig. 13 illustrates the relationships of the electromagnetic force in the x direction with the displacement in the x direction and control current in the y direction when the rotor of the RHMB with the new structure deviates from the balance position (x = 0 and y = 100 mm). As can be seen from the figure, the electromagnetic force in the x direction is basically linearly correlated with the displacement in the x direction; the control current in the y direction basically does not impair the electromagnetic force in the x direction. This further indicates that the hybrid magnetic fields of radial two DOFs along x and y directions in the designed RHMB are well decoupled. The linear variation of the force-displacement and force-current relationships can improve the control precision while reducing the difficulty of control.

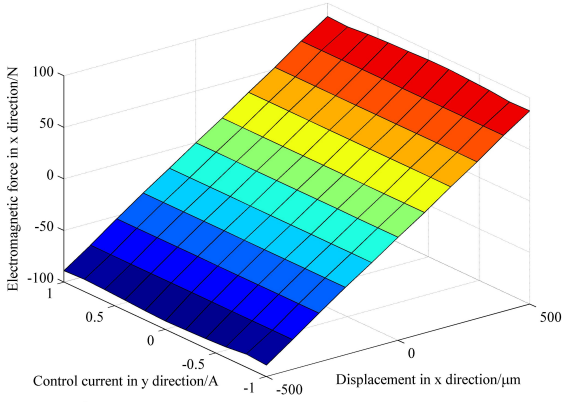

Fig. 13. Variation of the electromagnetic force in the x direction with the displacement in the x direction and control current in the y direction.

4.4. Core loss analysis

Conventional magnetic bearings with non independent stator cores in x and y direction, its bias magnetic circuit overlaps more with control magnetic circuit.When the coupling between bias magnetic flux and control magnetic flux is severe, it will increase the core loss. With the same main size parameters, the variation between the average core loss and the displacement of the rotor in x-direction generated by the decoupling model and the conventional model, is shown in Fig. 14. When the rotor return to its equilibrium position with the minimum control current required, the simulation values in the figure are obtained. when the load disturbance causes an increase displacement of rotor, core loss in the conventional model is significantly higher than that in the decoupled model. This is due to that the different magnetic circuit couples severely in conventional model, and the control magnetic intensity generated by the current is offset partly by the bias magnetic intensity, and

an additional increase in control current is required to push the rotor back to the equilibrium position.

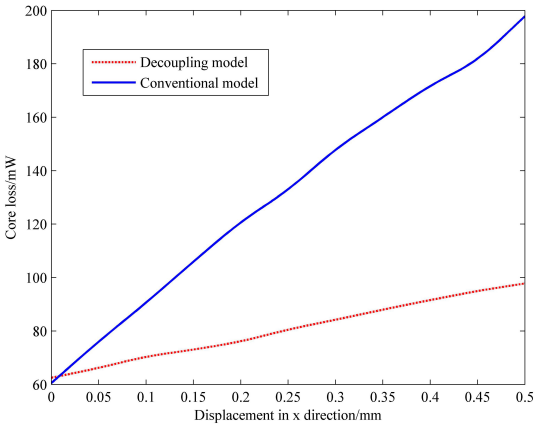

Fig. 14. Diagram of core loss.

When the rotor undergoes a displacement of 0.5mm, the main performance parameters of the two models are compared as shown in Table 2. The decoupling model reduces core loss by 50.12% compared to the conventional model, and the required control current is reduced from 2.3A to 1A. The decoupling model effectively solves the coupling problem between the bias magnetic circuit and the control magnetic circuit, and can effectively reduce the core loss and reduce the consumption of control current.

Table 2. Comparison of performance parameters between the two models.

	Average core loss (mW)	Minimum control current required (A)
Conventional model	197.8	2.3
Decoupling model	98.1	1

5. Conclusions

The research aims to solve magnetic circuit coupling of bias magnetic fluxes, radial magnetic fluxes, and control magnetic fluxes of radial two DOFs in RHMBs. To this end, a new RHMB having a mechanical structure with two independent stator cores separately set along x and y directions in the front and rear rows was designed. The equivalent magnetic circuit model was established and the analytical calculation formula for the electromagnetic force was derived. Then, 3D finite element simulation was conducted. The following conclusions are obtained through calculation and simulation:

1. The magnetic lines of force and cloud pictures of flux density distribution under excitation of the bias, control, and hybrid magnetic fields are completely consistent with the designed magnetic circuits of the new RHMB. The magnetic flux leakage is also low.

2. The analytical calculation results of the electromagnetic force based on the equivalent magnetic circuit model agree with the 3D finite element simulation results. The maximum errors of the two results for the force-displacement and force-current relationships are separately 3.77% and 6.63%.

3. The electromagnetic force in the x direction is positively proportional to the displacement in the x direction, while the displacement in the y direction hardly influences the electromagnetic force in the x direction. This indicates that the bias magnetic circuits in the x and y directions are well decoupled in the new RHMB. The electromagnetic force in the x direction has a linear relationship with the control current in the x direction, while it is basically not affected by the control current in the y direction. This suggests that the control magnetic fluxes in the x and y directions of the new RHMB are well decoupled. The electromagnetic force in the x direction is basically linearly related to the displacement in the x direction, while it is hardly influenced by the control current in the y direction, the decoupling model reduces core loss by 50.12% compared to the conventional model, indicative of good decoupling of the hybrid magnetic fields of radial 2 DOFs in the new RHMB. The research further proves that reasonable design of the mechanical structure can effectively solve magnetic circuit coupling of the RHMB. The force-displacement and force-current relationships are also well linearized, providing theoretical reference for the design and control of magnetic bearings.

Ackonowledgement

We acknowledge the support from the Natural Science Foundation of Gansu Province under grant No.22JR5RA383 and No.23JRRA919, the Innovation Fund Project of Education Department of Gansu Province under grant No.2022A-163 and 2023B-287, the Science and Technology Planing Project of Lanzhou City under grant No.2022-2-79.

References

[1] H. Zhu and S. Wang, (2020) *"Electromagnetic characteristics analysis and experiment study of six-pole radial-axial active magnetic bearing"* **Proceedings of the CSEE *40***(5): 1653–1663.

[2] Yang Bei,Zhang Ning,Zhang Haib,Li Qing,Wu Jihao, Li Jian, (2015) *"Design and simulation of radial active magnetic bearings"* **Cryogenics *43***(4): 31–35.

[3] Y. L. Zhong, L. J. Wu, X. Y. Huang, and Y. T. Fang, (2019) *"Nonlinear analytical model of heteropolar radial magnetic bearing"* **Zhejiang Daxue Xuebao (Gongxue Ban)/Journal of Zhejiang University (Engineering Science) *53***(1): 193–199. DOI: 10.3785/j.issn.1008-973X.2019.01.022.

[4] Lv Dongyuan, Lv Qichao, Li Yanbao,, Zhou Yiheng, Chen Xi, Jiang Yanfei, (2021) *"Design of Permanent Magnet Biased Magnetic Bearing for Magnetic Suspension Flywheel Energy Storage System"* **Flight Control Detection *4***(3): 76–81.

[5] L. Yong. *"Structural parameter design and control of double-plate radial-axial six-pole hybrid magnetic bearings, doctoral dissertation"*. (phdthesis). Jiangsu University, 2019.

[6] Duan Yijian. *"Twellve-pole heterpolar radial hybrid magnetic suspension bearings, doctoral dissertation"*. (phdthesis). Guilin University of Technology, 2021.

[7] Z. H. Zhou Jinyu, (2022) *"Development and Research Summary of Magnetic Bearings"* **Micromotors *55***(6): 93–98. DOI: 10.15934/j.cnki.micromotors.2022.06.003.

[8] X. Zhao, Z. Deng, and B. Wang, (2012) *"Parameter design and realization of permanent magnet biased heterploar radial magnetic bearing"* **Diangong Jishu Xuebao/Transactions of China Electrotechnical Society *27***(7): DOI: 10.19595/j.cnki.1000-6753.tces.2012.07.017.

[9] Yu Chunmin,Deng Zhiquan,Mei Lei, Pang Gucai, (2020) *"Research of New Hybrid Axial-Radial Magnetic Bearing Based on Accurate Magnetic Circuit"* **TRANSACTIONS OF CHINA ELECTROTECHNICAL SOCIETY *35(S1)***: 101–109. DOI: 10.19595/j.cnki.1000.

[10] M. A. Hossain. *"High temperature, permanent magnet biased, homopolar magnetic bearing actuator"*. (phdthesis). Texas A&M University, 2006.

[11] L. Jingyun. *"Electromagnetic characteristic analysis and research of uncoupled radial hybrid magnetic bearing for centrifugal pump"*. (phdthesis). Huaiyin Institute of Technology, 2022.

[12] M. Zong, T. Wu, and D. Wang, (2015) *"Feed-forward compensation decoupling control for hybrid radial magnetic bearing used in high speed electric machine"* **Diangong Jishu Xuebao/Transactions of China Electrotechnical Society *30***(14): 539–544.

[13] Q. Y. Zhong Zhixian, Cai Zhonghou, (2022) *"Decoupling Design and Analysis of a New Radial Hybrid Magnetic Bearing"* **Proceedings of the CSEE *42***(04): 1596–1606.

[14] D. Mohanraj, R. Aruldavid, R. Verma, K. Sathiyasekar, A. B. Barnawi, B. Chokkalingam, and L. Mihet-Popa, (2022) *"A Review of BLDC Motor: State of Art, Advanced Control Techniques, and Applications"* **IEEE Access *10***: 54833–54869. DOI: 10.1109/ACCESS.2022.3175011.

[15] D. Mohanraj, J. Gopalakrishnan, B. Chokkalingam, and L. Mihet-Popa, (2022) *"Critical Aspects of Electric Motor Drive Controllers and Mitigation of Torque Ripple - Review"* **IEEE Access *10***(July): 73635–73674. DOI: 10.1109/ACCESS.2022.3187515.

[16] M. Deepak, G. Janaki, and C. Bharatiraja, (2023) *"Design Switched Reluctance Motor Rotor Modification Towards Torque Ripple Analysis For EVs"* **Journal of Applied Science and Engineering (Taiwan) *26***(7): 951–960. DOI: 10.6180/jase.202307_26(7).0006.

[17] Y. Hu, L. Li, W. Guo, and X. Li, (2022) *"Support Stiffness of Magnetic Bearing Based on Unequal Magnetic Circuit Area Design Method"* **Xinan Jiaotong Daxue Xuebao/Journal of Southwest Jiaotong University *57***(3): 648–656. DOI: 10.3969/j.issn.0258-2724.20210888.

[18] L. Q. Cui Gang Yu Jianrong, (2023) *"Design and Analysis of Spherical Decoupling Permanent-Magnet Biased Magnetic Bearing"* **Machine Tool Hydraulics *50***(7): 82–86.